# The impact of trench defects in InGaN/GaN light emitting diodes and implications for the "green gap" problem

F. C.-P. Massabuau,[1,a)] M. J. Davies,[2] F. Oehler,[1] S. K. Pamenter,[1] E. J. Thrush,[1] M. J. Kappers,[1] A. Kovács,[3] T. Williams,[4] M. A. Hopkins,[5] C. J. Humphreys,[1] P. Dawson,[2] R. E. Dunin-Borkowski,[3] J. Etheridge,[4] D. W. E. Allsopp,[5] and R. A. Oliver[1]
[1]*Department of Materials Science and Metallurgy, University of Cambridge, 22 Charles Babbage Road, Cambridge CB3 0FS, United Kingdom*
[2]*Photon Science Institute, School of Physics and Astronomy, Alan Turing Building, University of Manchester, Manchester M13 9PL, United Kingdom*
[3]*Ernst Ruska-Centre for Microscopy and Spectroscopy with Electrons, Forschungszentrum Jülich GmbH, Leo-Brandt- Straße, D-52425 Jülich, Germany*
[4]*Monash Centre for Electron Microscopy, Monash University, Clayton Campus, VIC 3800, Australia*
[5]*Department of Electronic and Electrical Engineering, University of Bath, Bath BA2 7AY, United Kingdom*

(Received 16 June 2014; accepted 10 September 2014; published online 19 September 2014)

The impact of trench defects in blue InGaN/GaN light emitting diodes (LEDs) has been investigated. Two mechanisms responsible for the structural degradation of the multiple quantum well (MQW) active region were identified. It was found that during the growth of the p-type GaN capping layer, loss of part of the active region enclosed within a trench defect occurred, affecting the top-most QWs in the MQW stack. Indium platelets and voids were also found to form preferentially at the bottom of the MQW stack. The presence of high densities of trench defects in the LEDs was found to relate to a significant reduction in photoluminescence and electroluminescence emission efficiency, for a range of excitation power densities and drive currents. This reduction in emission efficiency was attributed to an increase in the density of non-radiative recombination centres within the MQW stack, believed to be associated with the stacking mismatch boundaries which form part of the sub-surface structure of the trench defects. Investigation of the surface of green-emitting QW structures found a two decade increase in the density of trench defects, compared to its blue-emitting counterpart, suggesting that the efficiency of green-emitting LEDs may be strongly affected by the presence of these defects. Our results are therefore consistent with a model that the "green gap" problem might relate to localized strain relaxation occurring through defects. © *2014 AIP Publishing LLC*. [http://dx.doi.org/10.1063/1.4896279]

A crucial point to consider in improving the performance of any opto-electronic device is to understand the impact of defects on light emission. III-Nitrides have a particularly high defect density. As well as the extensively studied threading dislocations[1] which appear at the surface of quantum well (QW) structures as V-pits,[2] other (less studied) defects can be observed at the surface of InGaN/GaN QW structures. Here, we focus on trench defects, in which a trench is seen to partially or completely enclose a region of material with altered emission properties, which have been reported in both InGaN/GaN[3–5] and AlInGaN/GaN[6] QW structures, and also in thick InGaN epilayers.[7] The sub-surface structure of this defect has been previously investigated and shown to consist of a basal-plane stacking fault (BSF) bounded by a vertical stacking mismatch boundary (SMB) which opens up at the surface into an array of coalescing pits, thus forming a trench.[3] Most studies reporting the presence of trench defects mainly focussed on the peculiar emission properties of the enclosed region, where an intense light emission at a longer wavelength (redshift) has often been observed.[4,5,8,9] However, reduced intensity[3] or blueshifted[10] emission has also been reported for QWs grown under certain conditions. The SMB itself appears to be a non-radiative recombination centre.[11] The overall impact of trench defects on light emitting diodes (LEDs) is not fully understood and has received very limited attention. A few studies on green LEDs have hinted that trench defects lead to inhomogeneities in the luminescence[12] or to reduced photoluminescence intensity.[8] Here, we report a direct observation of active region degradation by trench defects in blue LEDs. We demonstrate a negative impact of trench defects on LED efficiency and suggest that the implications of our findings may extend to a more significant detrimental effect on the efficiency of green LEDs, which may be a contributor to the so-called "green gap."[13]

Four blue-emitting five-period InGaN/GaN QW structures were grown by metal-organic vapour phase epitaxy (MOVPE) in a Thomas Swan 6 × 2 in. close-coupled showerhead reactor. Trimethylgallium (TMG), trimethylindium (TMI), bis(cyclopentadienyl)magnesium ($Cp_2Mg$), silane ($SiH_4$), and ammonia ($NH_3$) were used as precursors. Hydrogen ($H_2$) was used as the carrier gas for GaN growth and nitrogen ($N_2$) as the carrier gas for InGaN growth. Pseudo-substrates consisting of ca. 5 $\mu$m of GaN (of which 2 $\mu$m undoped and 3 $\mu$m Si-doped to $5 \times 10^{18}$ $cm^{-3}$) grown on c-plane sapphire with a miscut of $0.25 \pm 0.1°$ towards $(11\bar{2}0)$ were employed. The temperatures cited here are those of the susceptor, on which the wafers are placed during growth, as measured by emissivity corrected pyrometry (from Laytec). The InGaN QWs were grown at 755 °C

a)Electronic mail: fm350@cam.ac.uk.

 

for 216 s using a constant TMG flow of 1.5 sccm (or 4.4 $\mu$mol·min$^{-1}$), with two structures grown using a TMI flow of 120 sccm (or 9.6 $\mu$mol·min$^{-1}$) and two structures with a flow of 300 sccm (or 24.2 $\mu$mol·min$^{-1}$). Despite this use of different TMI flows, a constant indium composition of $(17 \pm 1)$% and QW thickness of $(2.5 \pm 0.3)$ nm are maintained throughout the set of samples, as determined by X-ray diffraction (XRD). After the growth of InGaN, a thin GaN capping layer of ca. 1 nm is deposited at 755 °C. The growth of another 1 nm of GaN continues while the temperature is ramped up to 860 °C and the rest of the barrier is grown at 860 °C until ca. 7.5 nm of GaN in total is grown. A final Mg-doped GaN layer (to $1\times10^{19}$ cm$^{-3}$) of ca. 130 nm is deposited at 960 °C in $H_2$ carrier gas on top of two of the QW structures (one grown using 120 sccm of TMI and one using 300 sccm), followed by an anneal at 780 °C for 20 min in a nitrogen atmosphere for acceptor activation, thus making an LED p-i-n structure. For simplicity, hereafter, we will refer to structures grown using 120 sccm of TMI as QW1 and LED1, and those grown using 300 sccm as QW2 and LED2. A second set of InGaN/GaN QW samples was also grown using the same growth method as described above, but with a TMI flow of 180 sccm (i.e., 14.4 $\mu$mol·min$^{-1}$) and an InGaN growth temperature varying between 690 °C and 780 °C, thus generating structures emitting between 520 nm and 400 nm.

The thickness and composition of the samples were assessed by XRD by performing an $\omega$-2$\theta$ scan along the 002 reflection, according to the method described by Vickers *et al.*[14] Atomic force microscopy (AFM) using a Veeco Dimension 3100 AFM in tapping mode was employed to explore the topography of the samples. The sub-surface structure of the LEDs was studied by high angular annular dark field scanning transmission electron microscopy (HAADF-STEM) in a Tecnai F20 microscope operating at 200 kV. The TEM cross-sectional samples were prepared by mechanical polishing followed by dimpling and $Ar^+$ ion milling. Finally, the optical properties of the structures were assessed by photoluminescence (PL) measurements. The structures were mounted, inclined at Brewster's angle to minimise the effects of Fabry-Perot interference oscillations on the PL spectra,[15] on the cold finger of a variable temperature closed-cycle helium cryostat. For the PL spectroscopy continuous wave excitation was provided by a HeCd laser source and the PL emission collected and dispersed within a 0.85 m single grating spectrometer. LED samples were processed into side-contacted structures as follows: mesas were formed with a $Cl_2$-Ar inductively coupled plasma etch, using $SiO_2$ as an etch mask. The transparent contacts to the p-type GaN were formed by e-beam evaporation of Ni/Au (7/7 nm) and were subsequently annealed at 500 °C for 5 min. The n-type GaN contacts were formed using electron beam evaporation of Ti/Al/Ni/Au (20/100/20/400 nm), as were the current spreading fingers on the thin Ni/Au contacts. Electroluminescence (EL) measurements were made on-wafer using a probe station equipped with tungsten needle probes to connect to the anode and cathode contacts on the LEDs. The optical system was aligned for maximum light collection by adjusting the position of a photodiode (mounted on a microscope) relative to the LED whilst driving the latter at a fixed current.

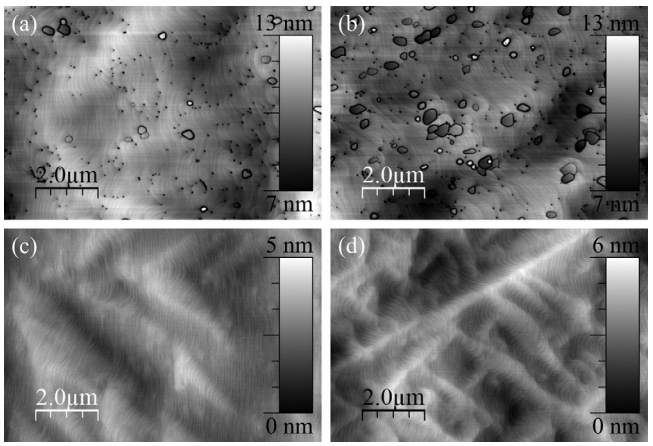


FIG. 1. AFM scans of the surface of QW1 (a), QW2 (b), LED1 (c), and LED2 (d).

The surface structure of the first set of samples, consisting of QW1, QW2, LED1, and LED2, can be seen in Figure 1. Trench defects can be observed at the surface of the QW structures (Figures 1(a) and 1(b)). As we have previously reported, the different TMI flow conditions we employed resulted in about an order of magnitude difference in trench defect density between the samples,[10] with densities of $(2 \pm 1) \times10^7$ cm$^{-2}$ and $(17 \pm 1) \times10^7$ cm$^{-2}$ for the structures grown at 120 sccm and 300 sccm, respectively. Interestingly, it should be noted that although trench defects are present at the surface of the QW structures, no such defect could be observed on the surface of the LED structures (Figures 1(c) and 1(d)).

The LEDs were observed in cross-section by HAADF-STEM along the $\langle 11\bar{2}0\rangle$ zone axis. This technique results in a Z-contrast image (also sensitive to strain), where InGaN, having a higher atomic number than GaN (and being more highly strained), appears brighter. The active regions of the two structures are compared in Figure 2. In both scans, the five QWs can be clearly identified as bright horizontal lines. LED2 exhibits additional features, arrowed in Figure 2(b). These features are similar to those seen by Li *et al.* who reported the observation of indium platelets and voids in QWs for green laser diodes, appearing as black and white regions in the active region and attributed them to active region thermal degradation.[16] It should be noted that no indium platelet or void could be observed in the QW structures grown without the p-type GaN layer (not shown here). This suggests that degradation of the active region is triggered by the growth of the p-type capping layer, as suggested by Li *et al.* Figure 3 presents another type of degradation of the InGaN QWs which is only observed in the LEDs. Figure 3

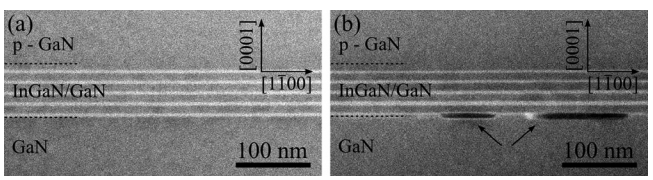


FIG. 2. HAADF-STEM pictures of LED1 (a) and LED2 (b), observed along $\langle 11\bar{2}0\rangle$. Indium platelets and voids can be observed in the first QWs of the stack in (b).

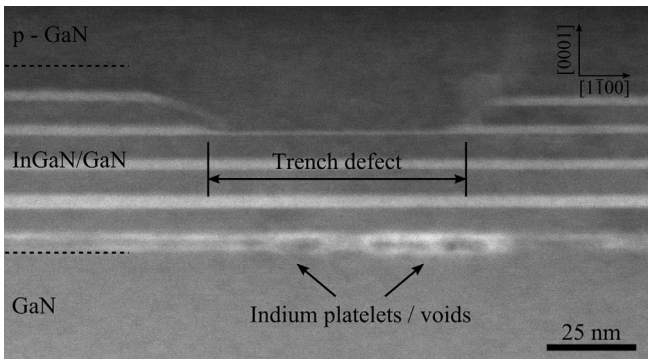


FIG. 3. HAADF-STEM picture of the LED2, observed along $\langle 11\bar{2}0 \rangle$. Besides the presence of indium platelets and voids in the lower part of the QW stack, the absence of QWs enclosed inside a trench defect can be observed.

shows the QW stack in LED2, with part of the fourth and fifth QWs missing. This region of missing active material is observed to be enclosed within a trench defect. Diffraction contrast imaging on the TEM (not shown here) confirmed the presence of the trench defect in various cases where missing QWs were seen, and a BSF could be observed (using the $\boldsymbol{g} = 1\bar{1}00$ diffraction condition[3]) beneath, but not necessarily directly below, the desorbed QWs. It is worth noting that the thermal degradation of the active region by indium platelets and voids only affects the first and occasionally the second QWs of the stack, while degradation by loss of active material in trench defects affects the top QWs.

Due to the systematic redshift of the luminescence originating from the enclosed region of trench defects,[11] it was initially thought that these areas had a much higher indium content, compensating the effect of strain relaxation of the QWs within the enclosed region. However, under certain growth conditions such as a relatively high TMI flow or elevated InGaN growth temperature, blueshifted luminescence from the enclosed regions was reported,[10] thus challenging the previous hypothesis. Based on the results reported in Ref. 10, the trench defects in the 300 sccm TMI grown structures (QW2 and LED2) are not expected to exhibit a significant luminescence redshift. (On ten-period QW samples emitting at 440 nm, Ref. 10 reported redshifts of $(1.7 \pm 0.3)$ nm for a structure grown with 300 sccm TMI compared to $(5.1 \pm 0.4)$ nm for a structure grown with 120 sccm TMI). Therefore, the indium content of the material enclosed within the trench is probably slightly higher than that of the surroundings, and just enough to compensate the blueshift resulting from the QW strain relaxation occurring within the enclosed region. The combination of increased composition together with different strain state in the QWs of the enclosed region might affect their thermal stability. Moreover, the presence of $H_2$ during the growth of the Mg-doped GaN at high temperature might aggravate the etching of the QWs, especially around the V-shaped ditch where the QWs are expected to be more exposed due to the thinner GaN barrier and the increased exposure time.

The light emission properties of the LEDs, containing high and low trench defect densities, were recorded by temperature dependent PL, and room temperature EL. Figure 4(a) shows the integrated PL intensity of the LEDs, measured for temperatures between 10 K and 300 K using an excitation power density of 13 W·cm$^{-2}$. At 10 K, the integrated PL intensities of the two devices were measured to be very similar, within a factor of two. The contribution of non-radiative recombination at 10 K is assumed to be negligible, and thus, we define the room temperature internal quantum efficiency (IQE) as the ratio of the integrated PL intensities measured at 10 K and 300 K.[17] A two order of magnitude reduction in room temperature IQE was measured for LED2 compared to LED1, with recorded IQEs of 0.015% and 5.5% respectively, when using an excitation power density of 13 W·cm$^{-2}$. With increasing excitation power density, up to approximately 350 W·cm$^{-2}$, the room temperature IQE of LED1 was measured to increase up to 45%, while LED2 increased only to 0.7%, as shown in Figure 4(b). The lower IQE recorded for LED2 relates to an increase in non-radiative recombination centres (linked to defects) within the structure.[18] The substantial difference in room temperature IQE, measured in the PL spectroscopy, for varying trench defect density was supported by room temperature EL measurements. Figure 4(c) shows the relative efficiency (i.e., photodiode current divided by the drive current) as a function of drive current for the two LEDs. Between 10 mA and 500 mA, the EL efficiency of LED1 was measured to be a minimum of two decades higher than that of LED2. The peak efficiency of LED1 was measured to occur at approximately 25 mA, while the efficiency of LED2 peaked for drive currents of about 250 mA. The carrier density at which the peak efficiency occurs is also believed to strongly relate to the density of defect-related non-radiative centres.[18] For drive currents below 10 mA, LED2 ceased to emit light,

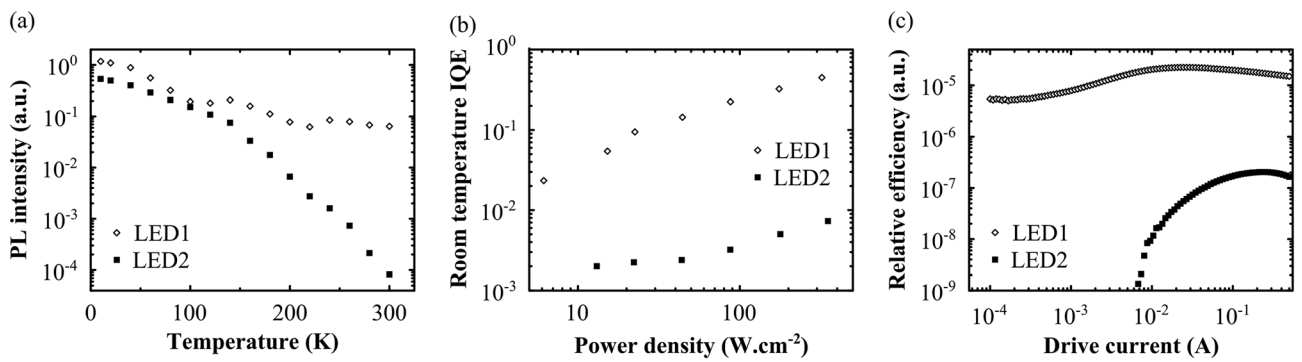


FIG. 4. (a) Integrated PL intensity determined by temperature dependent PL and (b) power dependent room temperature IQE measured by PL spectroscopy on LED1 and LED2. (c) Relative efficiency as a function of drive current measured by EL on 1 mm$^2$ devices.

while LED1 functioned for currents down to 0.1 mA, which may also reflect a variation in the density of non-radiative centres between the two structures. Given that the SMB has previously been associated with a non-radiative recombination centre,[11] we believe that the increase in the density of non-radiative recombination centres associated with the increase in trench defect density might relate to the SMBs. However, given that the number of non-radiative sites inserted into the structure varies for each trench defect, it is perhaps not surprising that the relationship between device efficiency and the density of trench defects appears to be non-linear. Moreover, the boundaries between the indium platelets observed in the lower QWs and the surrounding nitride material may also contribute to a high density of non-radiative centres. These two factors together might explain the overall large drop in efficiency.

In the second set of samples, with the QWs grown under constant TMI flow but varying temperature so that emission at different wavelengths was achieved, we note a two order of magnitude increase in trench defect density between blue- and green-emitting QW structures. This increase in density results in $(45 \pm 2)\%$ of the surface of the green-emitting structure (517 nm, 2.398 eV) being covered by trench defects, in comparison to the blue-emitting structure (448 nm, 2.767 eV) which has only $(3 \pm 1)\%$ of the surface covered (Figure 5). This result suggests that active region degradation by trench defects would be even more severe in green-emitting LEDs.

In Ref. 11, we suggested that the enclosed region of trench defects was relaxed due to the close proximity of the BSF and of the trench surrounding it. The high density of trench defects and the trench defect aggregates present at the surface of green structures (Figure 5(b)) would be expected to result in a greater local strain relaxation than in blue structures. Reciprocal space maps performed around the 006 and 204 reflections by XRD confirmed the presence of strain relaxation occurring in the QW structure emitting at 517 nm. Langer *et al*. attributed the origin of the green gap to strain-induced defects, where the strain relaxation was strongly localized around non-homogeneously distributed defects.[19] The picture suggested by Langer *et al*. seems to support our hypothesis on the influence of trench defects in green emitting samples.

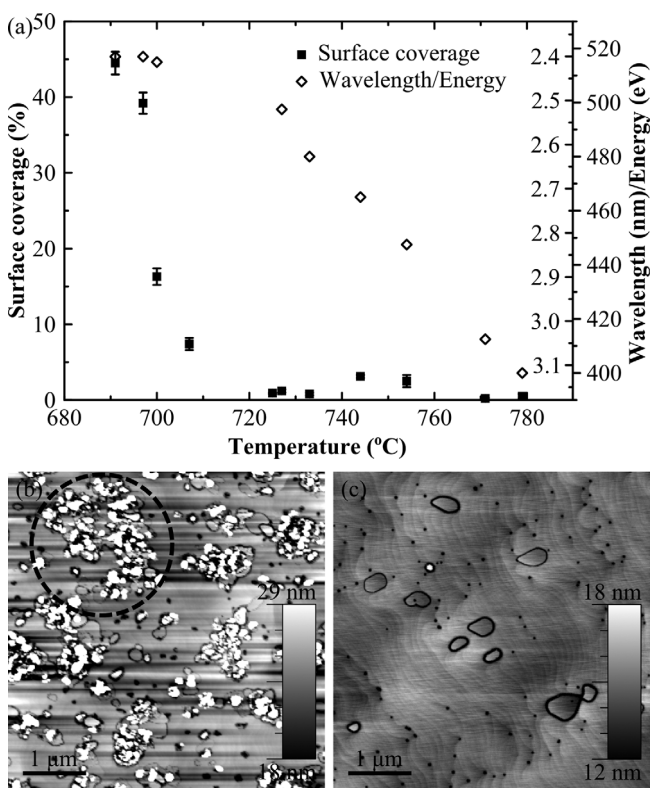


FIG. 5. (a) Trench defect surface coverage and room temperature PL peak emission plotted as a function of the InGaN growth temperature. 5 $\mu$m $\times$ 5 $\mu$m AFM scans of the surface of the QW structures emitting at 517 nm (b) and 448 nm (c). An aggregate of trench defects is circled in (b).

In conclusion, we investigated the impact of trench defects on the efficiency and structure of blue InGaN/GaN LEDs. Two mechanisms of active region degradation were identified. It was found that during the growth of the p-type capping layer, loss of part of the enclosed region of the trench defect occurs at the top part of the QW stack. Indium platelets and voids were also found to form preferentially at the bottom of the QW stack. The formation of trench defects resulted in a significant loss of efficiency of the LEDs, when measured by both PL and EL. The reduction in emission efficiency was attributed to an increase in the density of non-radiative recombination centres in the vicinity of the QW stack, likely associated with the SMBs. Investigation of the surface of green-emitting QW structures has revealed a density of trench defects up to two decades higher than measured for blue-emitting structures. We therefore suggest that the luminescence efficiency of green LEDs may be strongly affected by the presence of trench defects, consistent with a model that the green gap might relate to localized strain relaxation occurring through defects.

This work has been funded in part by the EPSRC (under EP/H0495331). The Tecnai F20 FEG-TEM at the Monash Centre for Electron Microscopy was funded by Australian Research Council Grant LE110100223.

[1]S. E. Bennett, Mater. Sci. Technol. **26**, 1017 (2010).
[2]N. Sharma, P. Thomas, D. Tricker, and C. J. Humphreys, Appl. Phys. Lett. **77**, 1274 (2000).
[3]F. C.-P. Massabuau, S.-L. Sahonta, L. Trinh-Xuan, S. Rhode, T. J. Puchtler, M. J. Kappers, C. J. Humphreys, and R. A. Oliver, Appl. Phys. Lett. **101**, 212107 (2012).
[4]J. Bruckbauer, P. R. Edwards, T. Wang, and R. W. Martin, Appl. Phys. Lett. **98**, 141908 (2011).
[5]S.-L. Sahonta, M. J. Kappers, D. Zhu, T. J. Puchtler, T. Zhu, S. E. Bennett, C. J. Humphreys, and R. A. Oliver, Phys. Status Solidi A **210**, 195 (2013).
[6]T. Suzuki, M. Kaga, K. Naniwae, T. Kitano, K. Hirano, T. Takeuchi, S. Kamiyama, M. Iwaya, and I. Akasaki, Jpn. J. Appl. Phys., Part 2 **52**, 08JB27 (2013).
[7]S. K. Rhode, W. Y. Fu, M. A. Moram, F. C.-P. Massabuau, M. J. Kappers, C. McAleese, F. Oehler, C. J. Humphreys, R. O. Dusane, and S.-L. Sahonta, J. Appl. Phys. **116**, 103513 (2014).
[8]S. M. Ting, J. C. Ramer, D. I. Florescu, V. N. Merai, B. E. Albert, A. Parekh, D. S. Lee, D. Lu, D. V. Christini, L. Liu, and E. A. Armour, J. Appl. Phys. **94**, 1461 (2003).
[9]M. S. Kumar, Y. S. Lee, J. Y. Park, S. J. Chung, C.-H. Hong, and E.-K. Suh, Mater. Chem. Phys. **113**, 192 (2009).
[10]F. C.-P. Massabuau, A. Le Fol, S. K. Pamenter, F. Oehler, M. J. Kappers, C. J. Humphreys, and R. A. Oliver, Phys. Status Solidi A **211**, 740 (2014).
[11]F. C.-P. Massabuau, L. Trinh-Xuan, D. Lodie, E. J. Thrush, D. Zhu, F. Oehler, T. Zhu, M. J. Kappers, C. J. Humphreys, and R. A. Oliver, J. Appl. Phys. **113**, 073505 (2013).

[12]T. Hikosaka, T. Shioda, Y. Harada, K. Tachibana, N. Sugiyama, and S.-Y. Nunoue, Phys. Status Solidi C **8**, 2016 (2011).
[13]S. Nakamura, M. Senoh, N. Iwasa, and S. Nagahama, Jpn. J. Appl. Phys. **34**, L797 (1995).
[14]M. E. Vickers, M. J. Kappers, T. M. Smeeton, E. J. Thrush, J. S. Barnard, and C. J. Humphreys, J. Appl. Phys. **94**, 1565 (2003).
[15]D. M. Graham, A. Soltani-Vala, P. Dawson, M. J. Godfrey, T. M. Smeeton, J. S. Barnard, M. J. Kappers, C. J. Humphreys, and E. J. Thrush, J. Appl. Phys. **97**, 103508 (2005).
[16]Z. Li, J. Liu, M. Feng, K. Zhou, S. Zhang, H. Wang, D. Li, L. Zhang, D. Zhao, D. Jiang, H. Wang, and H. Yang, Appl. Phys. Lett. **103**, 152109 (2013).
[17]S. Hammersley, D. Watson-Parris, P. Dawson, M. J. Godfrey, T. J. Badcock, M. J. Kappers, C. McAleese, R. A. Oliver, and C. J. Humphreys, J. Appl. Phys. **111**, 083512 (2012).
[18]J. Piprek, Phys. Status Solidi A **207**, 2217 (2010).
[19]T. Langer, H. Jonen, A. Kruse, H. Bremers, U. Rossow, and A. Hangleiter, Appl. Phys. Lett. **103**, 022108 (2013).